INTERNATIONAL JOURNAL OF STRUCTURAL CHANGES IN SOLIDS – Mechanics and Applications
Volume 1, Number 1, December 2009, pp. 149-170
IJSCS

A 3-species model for shape memory alloys

A.K. Nallathambi, S. Doraiswamy, A.S. Chandrasekar, S.M. Srinivasan*

Department of Applied Mechanics, Indian Institute of Technology Madras, Chennai, India-600036

Abstract

A thermodynamically consistent three species (austenite, plus-martensite & minus-martensite) model for shape memory alloys (SMA) is proposed. The uniaxial model proposed has been formulated with capabilities of simulating the characteristic response under general thermo-mechanical loading conditions. It is shown that a minimal set of model variables, essentially, the volume fractions of the three species, describing the one dimensional state of the polycrystal SMA, is enough to capture its characteristic features including the pseudoelastic and the shape memory effects. Primarily, two back stresses are defined within a dissipative setting - one to take care of polycrystalline nature of SMA and the other for the moving interfaces of the species within the sub grains. The connection between the physical response of the material and the choice of the material parameters is illustrated using different conditions of the material and of the loading. Simulation results exemplify the potential of the proposed model in predicting the characteristic behavior under loading paths such as isothermal, iso-stress and cyclic thermomechanical loading, that are typical in the applications.

1. Introduction

Due to the increased use of shape memory alloys (SMAs) under the combined thermal and mechanical loading, it is necessary to be able to predict their response under such conditions. SMAs show two characteristic responses to the applied thermomechanical loads called the pseudoelastic effect (PE) and the shape memory effect (SME). These are observed in several types of metallic materials and are being increasingly explored for various applications in the realm of aerospace, automotive and biomedical applications (Chopra, 2002). Other related phenomena seen in these materials include, two- way shape memory effect, cycling ageing and functional fatigue (Bernardini and Pence, 2002). In SMAs, the material undergoes a reversible phase transformation between the high symmetry parent phase, called the austenitic phase (A) and the low symmetry product phase, called the martensitic phase (M). The transformation results in large strains, typically up to 6%, and is observed over a reasonably small stress (and/or temperature) range (maintaining almost a constant transformation temperature and/or stress level). Typically, pseudoelasticity is observed to be a temperature dependent response and the observed strain recovery, in general, decreases with decrease in temperature. There is a significant difference in the loading and unloading responses leading to hysteresis. Since there is a recovery of strain, but still dissipation is involved, this behaviour is also referred to as pseudoelasticity. The large hysteresis is one of the key characteristics which make the SMA, a good choice for vibration damping (Smith, 2004). The other characteristic behaviour is the shape memory effect. This is seen over a minimum of two-steps involving both thermal and mechanical loading. Typically, the first step is a cooling process from the austenite phase to the martensite phase followed by a mechanical loading. Upon loading, a permanent set is seen in the martensite phase. The permanent set is recovered by heating it back to the austenite phase. This memory of the initial (parent) state is known as

*Corresponding author
Email address: mssiva@iitm.ac.in (S.M. Srinivasan)

the one way shape memory effect. It is to be noted that, after the recovery of the set, cooling (without stress) will not yield the deformed shape. In cases where such a recovery is seen, the response is termed as two-way shape memory effect (Lexcellent *et al.*, 2000). SME involves two different transformations, viz., from austenite to twinned martensite while cooling, and the 'detwinning' of the twinned martensite due to mechanical loading. The mechanical loading transforms one of the twins, leading ultimately to a state with a single 'variant' of martensite (for more information refer to Otsuka and Wayman (1998)).

An important area of active research is in the development of models capable of predicting the complex, hysteretic response of these materials under combined and arbitrary thermomechanical loading. Especially, in the usage of SMA in devices, this prediction helps in a better understanding leading to more efficient design. SMA devices undergo thermomechanical actuation cycles, intentional or otherwise, which involve partial or incomplete transformations. Most existing models capture the essential pseudoelastic and/or shape memory response, but often fail when it comes to modeling response under an arbitrary thermo-mechanical loading path (Seelecke and Muller, 2004).

In general, the models for SMA behavior have the following two salient aspects.

- the description of phase transformation in terms of evolution of martensitic fraction(s) as a function of driving forces viz., stress (σ) and temperature (T)- the evolution or phase kinetics, and,
- the constitutive behavior in terms of stress, temperature and strain (ϵ) using the phase fraction (ξ) as an internal state variable - the constitutive law.

Most of the models that describe the macroscopic SMA behavior can be classified as:

1. Free-energy or thermodynamics based models (Rajagopal and Srinivasa, 1999; Chenchiah and Sivakumar, 1999; Ivshin and Pence, 1994; Bernardini and Pence, 2002; Boyd and Lagoudas, 1996; Chang *et al.*, 2006)
2. Phenomenological models - plasticity or phase-diagram based (Bekker and Brinson, 1998; Lubliner and Auricchio, 1996; Lexcellent *et al.*, 2000; Kumar *et al.*, 2007), and,
3. Hysteresis models like the Preisach or the Duhem-Madelung models (Ortin, 1992).

Phenomenological models lack a physical basis and therefore have arbitrarily matched constants and parameters, which leads to cautious confidence among the users (Bekker and Brinson, 1998; Brinson, 1993). The parameters are generally described in an *ad hoc* manner and cannot always be systematically related to the material characteristics. This severely limits the necessary flexibility when working with these models. Also, depending on the requirements, more constants are arbitrarily added, making these models cumbersome (for example Buravalla and Khandelwal (2008)). On the other hand, plasticity based models use the principles of plasticity to model the dissipative phenomena associated with hysteretic responses. But, models of this category, thus far proposed in literature, work in an isothermal setting and therefore, suffer severely under complex thermomechanical loading (Lubliner and Auricchio, 1996).

In a thermodynamic framework, it becomes convenient to handle both thermo-mechanical loading and hysteretic response and can lead to simple generalized plasticity type models. There are several models which have been developed in this fashion. However, the choice of variables and the appropriate modeling has a lot of bearing in correctly modeling the material characteristics. Some of the existing models lead to certain inadequacies and inconsistencies (Boyd and Lagoudas, 1996; Shub and Lagoudas, 1999). Shaw and coworkers (Chang *et al.*, 2006) have proposed a model involving kinetics of the phase-front which is unsuitable for a lumped parameter modeling approach. The model requires solving an initial boundary value problem for even the simplest of the cases of SMA response. While, such a formulation may be useful in a setting where only avalanching softening occurs, in a stabilized polycrystalline SMA, such a formulation adds unnecessary rigor from a design tool perspective. The model proposed by Lagoudas and coworkers (Shub and Lagoudas, 1999; Boyd and Lagoudas, 1996), are thermodynamics based models. However, in handling combined psuedoelastic and shape memory effect that usually occurs under a general thermo-mechanical loading, the evolution of the material parameters are not consistent with the thermodynamic laws and therefore, may lead to problems related to response under general thermo-mechanical loading. The models developed by Pence and coworkers (Ivshin and Pence, 1994; Bernardini and Pence, 2002), reduce the kinetics to a single variable evolution that puts too much constraint on modeling the general thermomechanical response.

There exists a wide conceptional modelling gap between the two extreme properties of SMA (SME and PE). Combined thermomechanical loading path can be treated as a good test case for an efficient model. A model which handles the thermomechanical loading path deftly and predicts the SMA response convincingly is not yet a reality in the research community. This work presents a thermodynamically consistent, dissipation based three species model for SMA. The three species introduced in this model are: austenite, plus-martensite and minus-martensite. The plus and minus martensite introduced in this model should not be directly compared with the twinned and detwinned martensite. Their definitions are discussed in Section 2. The proposed thermodynamic framework, attempts a simple one dimensional lumped parameter model for a stabilized polycrystalline wire form of SMA. In essence, the framework tries to capture the response with a model consisting of a minimal set of variables and, at the same time, simulates complex thermo-mechanical behavior consistent with physically admissible transformation kinetics. This helps in providing a valuable insight while conducting characteristic tests on the wire, avoiding redundant tests.

In the first part of Section 2, the thermodynamic formulation and the model, right from the definition of state to the driving force relations, are discussed. The driving forces are functions of the state variables and provide the kinetics of the evolution of phases. The driving force equations are obtained as a direct consequence of the mechanical dissipation inequality arising out of the second law of thermodynamics. The evolution equations, the flow rule, the hardening rules and the consistency conditions are presented in the later part of Section 2. In Section 3, the role of the parameters involved in this model are explained with the help of phase diagrams. Three different phase diagrams are constructed for three different cases of illustration: no dissipation - no hardening case, dissipation with no hardening and dissipation with hardening. Computational aspects of this model are discussed in Section 4 before presenting the the simplifications and assumptions required for simulations in Section 5. Simulation results are presented in Section 6 and it is shown that the prediction is quite satisfactory even for a simplistic assumption. Specific cases are discussed to bring out the versatility and the efficacy in the model.

2. Thermodynamical framework of the model

The overall objective of developing a thermodynamic framework is to be able to simulate the quasistatic behavior of SMA. The constitutive models developed within this framework should be capable of, within a hierarchical framework, simulating all the characteristic quasistatic behavior of the shape memory alloys such as shape memory effect, pseudoelastic effect, strain-rate dependence, cyclic ageing and functional fatigue. In the hierarchy of inclusion of effects in the framework, the first attempt is on the quasistatic modeling of pseudoelastic and shape memory effects. Since the devices work well within the complete transformation conditions, it is important to consider partial cycles of mechanical loading and unloading, as well as, heating and cooling. Upon developing the model, appropriate numerical schemes are necessary to simulate the behavior.

The pseudoelastic effect as described in the previous section is an isothermal transformation from austenite to detwinned martensite. On the other hand, the shape memory effect involves 'detwinning' of twinned martensite, the heating of which transforms it into the parent phase (austenite). Therefore, there is a transformation which involves three distinct states. In other words, with three variables to express the state/phase of the material, the description can be deemed complete. Therefore, this model has been defined on a three species partitioning of the phases in the material.

The three species defined are austenite (A), plus-martensite (M^+) and minus-martensite (M^-). Plus-martensite is the projection of the variants that exist in a completely detwinned state under tension, and minus-martensite is the projection of the variants that exist in the completely detwinned state under compression. The state of the material is assumed to be completely defined by the stress (σ), temperature (θ), the austenite volume fraction (α) and the two martensite volume fractions, (ξ^+ and ξ^-). The two martensite species M^+ and M^- considered in this work are not directly equivalent to the twinned and the detwinned martensites well established in the literature Brinson (1993).

Certain combinations of (M^+) and (M^-) could represent the twinned and the detwinned martensite states as shown in Fig. 1 Roubicek (2004).

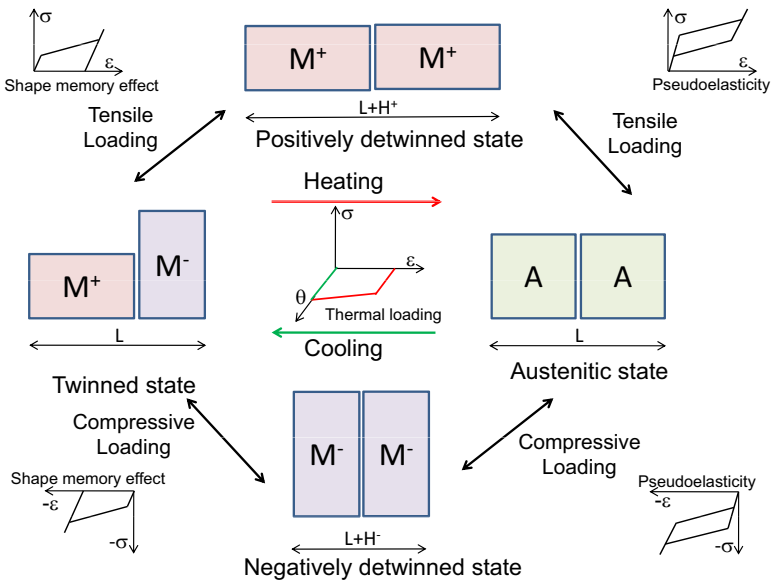

Figure 1: Representing the twinned and detwinned states of SMA interms of austenite (A), plus-martensite (M^+) and minus-martensite(M^-)

In this work, Gibbs free energy is used to define the free energy at each state. Since the thermodynamic state of the material is defined completely by stress, temperature and the species volume fractions, the Gibbs free energy is also completely known at any state as a function of the state variables. The dissipation that occurs in the material should satisfy the mechanical dissipation inequality, which guarantees that the second law of thermodynamics is satisfied. From the Gibbs energy equation of state, we get the evolution kinetics of the species involved during a transformation. The model is complete once we know the evolution kinetics of the species. The model is developed in a rate-independent setting.

Given that at any given time, the state of the material within a representative volume, the volume fractions of the three species, A, M^+ and M^- are connected through the rule of mixtures as,

$$\alpha + \xi^+ + \xi^- = 1, \tag{1}$$

the rate of change of volume fractions can be derived as,

$$\dot{\alpha} + \dot{\xi}^+ + \dot{\xi}^- = 0. \tag{2}$$

The total strain (ϵ) can be additively decomposed into the elastic strain, (ϵ^e), and the transformation strain, (ϵ^t), since we are dealing with reasonably small deformations in this formulation. Thus,

$$\dot{\epsilon} = \dot{\epsilon}^e + \dot{\epsilon}^t \tag{3}$$

The transformation strain, ϵ^t is produced during transformations between the austenite and both the martensite phases. It is assumed that the plus-martensite produces positive transformation strains, while the minus-martensite produces negative transformation strains. The total transformation strain rate, $\dot{\epsilon}^t$, is assumed to be additively composed of the M^+ transformation strain rate, $\dot{\epsilon}^{+t}$, and the M^- transformation strain rate, $\dot{\epsilon}^{-t}$, such that,

$$\dot{\epsilon}^t = \dot{\epsilon}^{+t} + \dot{\epsilon}^{-t} \tag{4}$$

The transformation strain rates, $\dot{\epsilon}^{+t}$ and $\dot{\epsilon}^{-t}$, are assumed to evolve with respect to the respective volume fraction rates as,

$$\dot{\epsilon}^{+t} = H^{+}\dot{\xi}^{+} \tag{5}$$
$$\dot{\epsilon}^{-t} = H^{-}\dot{\xi}^{-} \tag{6}$$

where H^+ and H^- are, respectively, maximum uniaxial transformation strain produced under tensile and compressive loading. These parameters, though assumed to be constants, can be nonlinear functions of the state variables, ξ^+ and ξ^- constrained by the condition that at the limits of the volume fraction variables, the maximum transformation strains are realized. The Gibbs free energy density of the mixture of the three species is assumed to be completely defined by the specification of the volume fractions of the three species and the external drivers: the stress, σ and the temperature, θ. In this, a strong assumption is made in that the the interface energies can be fully prescribed in terms of the volume fractions. This assumption, however, is acceptable since the we are dealing with a macroscopic behavior that in a sense smears the bulk and the interfacial behavior Guthikonda *et al.* (2008). The innate assumption is that the interfaces are densely populated at all values of the volume fractions. This model breaks down only at values of the volume fractions that are close to the limits. Thus, we assume that, the Gibbs free energy is defined by,

$$G := G(\sigma, \theta, \alpha, \xi^{+}, \xi^{-}) \tag{7}$$

As mentioned in the above, the total Gibbs free energy density, G, is composed of contributions from the bulk, G^b and the free energy stored in the interfaces (or surfaces), G^s, so that,

$$G = G^{b} + G^{s} \tag{8}$$

The bulk Gibbs free energy of all the grains, G^b within the representative volume is the volume average of the austenite Gibbs free energy, G^{α}, the plus-martensite Gibbs free energy, $G^{\xi+}$, and minus-martensite Gibbs free energy, $G^{\xi-}$. Therefore, the bulk Gibbs free energy, G^b is given by,

$$G^{b} = \alpha G^{\alpha} + \xi^{+} G^{\xi^{+}} + \xi^{-} G^{\xi^{-}} \tag{9}$$

In this framework, the interface energy G^s, is decomposed further, for the sake of linking with the physical mechanism of transformation, into the grain orientation energy, G^o and the subgrain interface energy, G^i. This helps in separating the inter granular mechanisms and the subgrain related mechanisms of transformation between the three species. Thus,

$$G^{s} = G^{o} + G^{i} \tag{10}$$

G^o is the energy associated with the initial disposition of the grains in terms of the orientations of the austenitic grains in the polycrystalline material. The corresponding orientations of plus- and minus-martensites primarily contribute to the transformation strain. Therefore, G^o is treated as a function of transformation strain (ϵ^t) only. This leads to

$$G^{o} := G^{o}(\epsilon^{t}). \tag{11}$$

The interaction energy at the interfaces of the plus-martensite and the minus-martensite are assumed to be negligible compared to the austenite-martensite interaction energy. Thus, the Gibbs free energy due to interaction (G^i) of austenite and martensite is taken to be a function of α only. When $\alpha = 0$, this interaction energy is zero, because the only phase present is the martensite phase (either plus or minus or, a combination of plus and minus). Similarly when $\alpha = 1$, the interaction energy is zero, since only austenite is present. Therefore,

$$G^{i} := G^{i}(\alpha) \tag{12}$$

Putting all the above together, the constitutive form of the total specific Gibbs free energy of polycrystalline SMA can now be written in terms of the external variables σ and θ and the internal variables α, ξ^+ and ξ^- as,

$$G = G(\sigma, \theta, \alpha, \xi^{+}, \xi^{-}) = \alpha G^{\alpha} + \xi^{+} G^{\xi^{+}} + \xi^{-} G^{\xi^{-}} + G^{o}(\epsilon^{t}) + G^{i}(\alpha) \tag{13}$$

Specific Gibbs free energy of the individual phases, the austenite or the martensite phases, can be taken as functions of stress, σ and temperature, θ, such that

$$G^{\alpha} = G^{\alpha}(\sigma) + G^{\alpha}(\theta) \tag{14}$$

$$G^{\xi^{+,-}} = G^{\xi^{+,-}}(\sigma) + G^{\xi^{+,-}}(\theta) \tag{15}$$

In order to satisfy the second law of thermodynamics, the mechanical dissipation is defined in terms of internal energy, u, so that the dissipation inequality, Δ can be written as in Rajagopal and Srinivasa (1999),

$$\Delta := \sigma\dot{\epsilon} - \rho\dot{u} - \rho\dot{\eta}\theta \geq 0 \tag{16}$$

where ρ is the mass density. Note here that if equation (16) is satisfied, then the second law of thermodynamics is guaranteed to be satisfied. Introducing the relation between the Gibbs free energy, G and internal energy, u, to be $u = G + \eta\theta + \sigma\epsilon$, and it's functional form as described above, taking time derivative of u, and from the definition of entropy (η), the dissipation inequality in (16) is reduced to

$$-\left(\epsilon^{e} + \rho\frac{\partial G}{\partial \sigma}\right)\dot{\sigma} - \left(\rho\epsilon^{t} + \rho\frac{\partial G}{\partial \theta}\right)\dot{\theta} + \left[\sigma H^{+} - \rho\frac{\partial G}{\partial \xi^{+}}\right]\dot{\xi}^{+} + \left[\sigma H^{-} - \rho\frac{\partial G}{\partial \xi^{-}}\right]\dot{\xi}^{-} + \left[-\rho\frac{\partial G}{\partial \alpha}\right]\dot{\alpha} \geq 0 \tag{17}$$

Thus, using the admissibility condition of the internal states, the following constitutive relations between the arguments and their conjugates are arrived at.

$$\epsilon^{e} = -\rho\frac{\partial G}{\partial \sigma} \tag{18}$$

$$\rho\eta = -\frac{\partial G}{\partial \theta}. \tag{19}$$

The dissipation inequality further reduces to

$$\left[\sigma H^{+} - \rho\frac{\partial G}{\partial \xi^{+}}\right]\dot{\xi}^{+} + \left[\sigma H^{-} - \rho\frac{\partial G}{\partial \xi^{-}}\right]\dot{\xi}^{-} + \left[-\rho\frac{\partial G}{\partial \alpha}\right]\dot{\alpha} \geq 0. \tag{20}$$

Upon inserting the derivatives of Gibbs free energy with respect to α, ξ^{+} and ξ^{-}, the final form of the inequality becomes,

$$\left[\sigma H^{+} - \rho G^{+} - \rho\frac{\partial G^{o}}{\partial \xi^{+}}\right]\dot{\xi}^{+} + \left[\sigma H^{-} - \rho G^{-} - \rho\frac{\partial G^{o}}{\partial \xi^{-}}\right]\dot{\xi}^{-} + \left[-\rho G^{\alpha} - \rho\frac{\partial G^{i}}{\partial \alpha}\right]\dot{\alpha} \geq 0 \tag{21}$$

$$\text{or, } \Delta = f^{+}\dot{\xi}^{+} + f^{-}\dot{\xi}^{-} + f^{\alpha}\dot{\alpha} \geq 0 \tag{22}$$

where the driving forces f^{+}, f^{-} and f^{α} corresponding to M^{+}, M^{-} and α species volumes respectively, are given by,

$$f^{+} = \sigma H^{+} - \rho G^{+} - \rho\frac{\partial G^{o}}{\partial \xi^{+}} \tag{23}$$

$$f^{-} = \sigma H^{-} - \rho G^{-} - \rho\frac{\partial G^{o}}{\partial \xi^{-}} \tag{24}$$

$$f^{\alpha} = -\rho G^{\alpha} - \rho\frac{\partial G^{i}}{\partial \alpha} \tag{25}$$

Summarizing the above mentioned relations,

$\Delta = f^{+}\dot{\xi}^{+} + f^{-}\dot{\xi}^{-} + f^{\alpha}\dot{\alpha} \geq 0$	dissipation inequality
$\alpha + \xi^{+} + \xi^{-} = 1$	species constraint
$\dot{\alpha} + \dot{\xi}^{+} + \dot{\xi}^{-} = 0$	species evolution constraint

While solving the dissipation inequality in eq. (22), the species and species evolution constraints have to be taken into consideration as indicated in the above box. The evolution kinetics of the various species involved in a particular transformation can be derived from eq. (22). The possible transformations are $A \leftrightarrow M^+$, $A \leftrightarrow M^-$ and $M^- \leftrightarrow M^+$.

Considering a specific example of transformation, where the austenite is involved in the transformation,

- When $\dot{\alpha} \neq 0$, $\dot{\alpha} = -\dot{\xi}^+ - \dot{\xi}^-$, eq. (22) becomes,

$$(f^+ - f^\alpha)\dot{\xi}^+ + (f^- - f^\alpha)\dot{\xi}^- \geq 0 \tag{26}$$

  Assuming a form for the mechanical dissipation for each of the volume fraction rates, $\dot{\xi}^+$ and $\dot{\xi}^-$, we have,

$$k_1 \left|\dot{\xi}^+\right| + k_2 \left|\dot{\xi}^-\right| \geq 0 \tag{27}$$

  Since $\dot{\xi}^+$ and $\dot{\xi}^-$ are independent in this case, each of the terms in the above dissipation inequality should satisfy the inequality individually. i.e.,

$$(f^+ - f^\alpha)\dot{\xi}^+ \geq 0 \text{ and } (f^- - f^\alpha)\dot{\xi}^- \geq 0 \tag{28}$$

  and using the form of dissipation given in eq. (27), we can write,

$$\begin{array}{llll} |f^+ - f^\alpha| = k_1 & \text{for} & \dot{\xi}^+ \neq 0 & \text{and} \\ |f^- - f^\alpha| = k_2 & \text{for} & \dot{\xi}^- \neq 0. & \end{array}$$

  if both constraints are satisfied, both $\dot{\xi}^+$ and $\dot{\xi}^-$ are non-zero, where transformations occur at the expense of α. In general, k_1 and k_2 can be functions of the current state.

- For the special case when $\dot{\alpha} = 0$, the constraint in eq. (2) becomes,

$$\dot{\alpha} = -\dot{\xi}^+ - \dot{\xi}^- \implies \dot{\xi}^- = -\dot{\xi}^+ \tag{29}$$

  Note that, this case has meaning only if $\dot{\alpha} = 0$. Therefore, for this case, eq. (22) becomes,

$$(f^+ - f^-)\dot{\xi}^+ \geq 0 \tag{30}$$

  so that, $\dot{\xi}^+ \neq 0$, when $|f^+ - f^-| = k_3$, assuming a form of mechanical dissipation similar to the one used in eq. (27). Again, here, k_3 can be a function of the current state of the material.

In general, all the conditions can be grouped with their corresponding evolution conditions as,
$\dot{\alpha} \neq 0$, if

$$\begin{array}{rcl} \left|f^+ - f^\alpha\right| & = & k_1 \\ \quad and/or & & \\ \left|f^- - f^\alpha\right| & = & k_2 \end{array} \tag{31}$$

$\dot{\xi}^+ \neq 0$, if

$$\begin{array}{rcl} \left|f^+ - f^\alpha\right| & = & k_1 \\ \quad and/or & & \\ \left|f^+ - f^-\right| & = & k_3 \end{array} \tag{32}$$

$\dot{\xi}^- \neq 0$, if

$$\begin{aligned} \left|f^- - f^\alpha\right| &= k_2 \\ \quad and/or & \\ \left|f^+ - f^-\right| &= k_3 \end{aligned} \tag{33}$$

Define the driving force $D^{\alpha+}$ as $D^{\alpha+} = f^+ - f^\alpha$. Upon substitution from the equations (23), (24), and (25), we get,

$$D^{\alpha+} = \sigma H^+ + \rho \Delta G^{+\alpha} - \rho \frac{\partial G^o}{\partial \xi^+} + \rho \frac{\partial G^i}{\partial \alpha} \tag{34}$$

In a similar way the other driving forces can be written as,

$$D^{\alpha-} = \sigma H^- + \rho \Delta G^{-\alpha} - \rho \frac{\partial G^o}{\partial \xi^-} + \rho \frac{\partial G^i}{\partial \alpha} \tag{35}$$

$$D^{-+} = \sigma (H^+ - H^-) + \rho \Delta G^{+-} - \rho \frac{\partial G^o}{\partial \xi^+} + \rho \frac{\partial G^o}{\partial \xi^-} \tag{36}$$

where

$$\begin{aligned} \Delta G^{+\alpha} &= G^\alpha - G^{\xi^+} \\ \Delta G^{-\alpha} &= G^\alpha - G^{\xi^-} \\ \Delta G^{+-} &= G^{\xi^-} - G^{\xi^+} \end{aligned}$$

As a first approximation, the maximum uniaxial transformation strain obtained in SMA under tensile and compressive loading can be assumed to be equal in magnitude, and therefore,

$$H^+ = -H^- = H, \text{ say} \tag{37}$$

The Gibbs free energy of plus-martensite and minus-martensite can be taken as equal because, the plus and minus martensite are species of the same phase (refer Section 5 for further specializations). Therefore,

$$G^{\xi^+} = G^{\xi^-} = G^\xi, \text{ say} \tag{38}$$

Then, the driving force equations can be rewritten in terms of H and $\Delta G^{\xi\alpha}$ $(= G^\alpha - G^\xi)$, as,

$$D^{\alpha+} = \sigma H + \rho \Delta G^{\xi\alpha} - \rho H \frac{\partial G^o}{\partial \epsilon^t} + \rho \frac{\partial G^i}{\partial \alpha} \tag{39}$$

$$D^{\alpha-} = -\sigma H + \rho \Delta G^{\xi\alpha} + \rho H \frac{\partial G^o}{\partial \epsilon^t} + \rho \frac{\partial G^i}{\partial \alpha} \tag{40}$$

$$D^{-+} = 2H \left(\sigma - \rho \frac{\partial G^o}{\partial \epsilon^t} \right) \tag{41}$$

In order to bring these expressions to a simple form, the above driving forces are normalized with respect to H so that they reduce to stress like terms and hence become,

$$\bar{D}^{\alpha+} \left(\xi^+, \alpha\right) = \sigma + \sigma^{\xi\alpha} - \beta^{\epsilon^t} + \beta^\alpha \tag{42}$$

$$\bar{D}^{\alpha-} \left(\xi^-, \alpha\right) = -\sigma + \sigma^{\xi\alpha} + \beta^{\epsilon^t} + \beta^\alpha \tag{43}$$

$$\bar{D}^{-+} \left(\xi^+, \xi^-\right) = 2 \left(\sigma - \beta^{\epsilon^t} \right) \tag{44}$$

where, $\sigma^{\xi\alpha} = \frac{\rho}{H}\Delta G^{\xi\alpha}$, $\beta^{\epsilon^t} = \rho\frac{\partial G^o}{\partial \epsilon^t}$, and $\beta^{\alpha} = \frac{\rho}{H}\frac{\partial G^i}{\partial \alpha}$.

Note that $\sigma^{\xi\alpha}$ is a function of the external force variables σ and θ. This term $\sigma^{\xi\alpha}$ arises due to two effects. One due to the difference in compliance between the austenite and martensite phases (considered as σ^C) and the other due to the latent heat of transformation between the austenite and the martensite phases (named as σ^L). Thus, the effect of $\sigma^{\xi\alpha}$ can be decoupled into two terms, each a function of a single external force variable, σ or θ. Therefore,

$$\sigma^{\xi\alpha} = \sigma^C + \sigma^L \tag{45}$$

where $\sigma^C = -\frac{\rho}{H}\Delta G^{\xi\alpha}(\sigma)$ a,nd $\sigma^L = -\frac{\rho}{H}\Delta G^{\xi\alpha}(\theta)$. The latent heat related term σ^L can be determined through experiments and is a function of only the temperature, θ. The back stresses (β^{ϵ^t}, β^{α}) are functions of internal variables ξ^+, ξ^- and α. In the elastic regions, the back stresses remain constant (or, in other words, the rate of change of these of these backstress is zero). With transformation, the back stresses evolve since they are dependent on the phase fractions. Thus, in the functional form, we have

$$\sigma^C = \sigma^C(\sigma) \tag{46}$$
$$\sigma^L = \sigma^L(\theta) \tag{47}$$
$$\beta^{\epsilon^t} = \beta^{\epsilon^t}(\epsilon^t) \tag{48}$$
$$\beta^{\alpha} = \beta^{\alpha}(\alpha) \tag{49}$$

and the complete transformation conditions can be summarized as

$\dot{\alpha} \neq 0,$	if	$\lvert D^{\alpha+}\rvert = k_1$	and / or	$\lvert D^{\alpha-}\rvert = k_2$
$\dot{\xi}^+ \neq 0,$	if	$\lvert \bar{D}^{\alpha+}\rvert = \bar{k_1}$	and / or	$\lvert \bar{D}^{-+}\rvert = \bar{k_3}$
$\dot{\xi}^- \neq 0,$	if	$\lvert \bar{D}^{\alpha-}\rvert = \bar{k_2}$	and / or	$\lvert \bar{D}^{-+}\rvert = \bar{k_3}$

where $\bar{k_1}$, $\bar{k_2}$ and $\bar{k_3}$ are dissipations for transformations, $\alpha \leftrightarrow \xi^+$, $\alpha \leftrightarrow \xi^-$ and $\xi^- \leftrightarrow \xi^+$ respectively.

For any thermomechanical loading, one has to check all the three transformation conditions. From this, the conclusion can be made on the possibilities of evolution of each of the species. This is discussed in section 4. The three dissipation potentials corresponding to the three driving forces, $\bar{D}^{\alpha+}$, $\bar{D}^{\alpha-}$, and $\bar{D}^{-+}$ can be written in a simple convex quadratic form as (as an example),

$$\Phi^{\alpha+} = \frac{1}{2}\left(\bar{D}^{\alpha+}\right)^2 \tag{50}$$
$$\Phi^{\alpha-} = \frac{1}{2}\left(\bar{D}^{\alpha-}\right)^2 \tag{51}$$
$$\Phi^{-+} = \frac{1}{2}\left(\bar{D}^{-+}\right)^2 \tag{52}$$

The evolution of the two state variables, ξ^+ and ξ^- for the rate independent case, can be expressed as

$$\dot{\xi}^+ = \dot{\lambda}^+\frac{\partial \Phi^{\alpha+}}{\partial \xi^+} \tag{53}$$
$$\dot{\xi}^- = \dot{\lambda}^-\frac{\partial \Phi^{\alpha-}}{\partial \xi^-} \tag{54}$$

Note that there are two transformation strain rate parameters, $\dot{\lambda}^+$ and $\dot{\lambda}^-$, arising here indicating that the 'flow' or transformation rule is connected as a vector field within the volume fraction admissibility constraints.

2.1. Evolution equations for the species

To start with, the simultaneous evolution of the species, α, ξ^+ and ξ^- under a thermo-mechanical loading is discussed here. In order to find out the occurrence of the transformations: $\alpha \leftrightarrow \xi^+$ and $\alpha \leftrightarrow \xi^-$, three different conditions have to be checked.

Following the principles of classical plasticity Hill (1950), the transformation strain can be determined from the systematic application of the transformation criteria, the loading criteria, the flow rules, the hardening rules and the consistency conditions.

Firstly, the following two transformation criteria have to be satisfied for the corresponding transformation to occur.

$$F_1 = \left|\bar{D}^{\alpha+}\right| - \bar{k_1} \Rightarrow F_1\left(\sigma,\theta,\xi^+,\xi^-,\alpha\right) = \left|\sigma + \sigma^{\xi\alpha} - \beta^{\epsilon^t} + \beta^{\alpha}\right| - \bar{k_1} = 0 \tag{55}$$

$$F_2 = \left|\bar{D}^{\alpha-}\right| - \bar{k_2} \Rightarrow F_2\left(\sigma,\theta,\xi^+,\xi^-,\alpha\right) = \left|-\sigma + \sigma^{\xi\alpha} + \beta^{\epsilon^t} + \beta^{\alpha}\right| - \bar{k_2} = 0 \tag{56}$$

Secondly, the volume fractions of each of the species should be between zero and unity.Thirdly, the loading criteria have to be satisfied.

All these can be summarized as,

Elastic region	:	$F_1 < 0$	and	$F_2 < 0$
Transformation zone	:	$F_1 = 0$	and	$F_2 = 0$
Forward transformation	:	$F_1 = 0$	and	$\frac{\partial \bar{D}^{\alpha+}}{\partial\sigma}\dot{\sigma} + \frac{\partial \bar{D}^{\alpha+}}{\partial\theta}\dot{\theta} > 0$
	:	$F_2 = 0$	and	$\frac{\partial \bar{D}^{\alpha-}}{\partial\sigma}\dot{\sigma} + \frac{\partial \bar{D}^{\alpha-}}{\partial\theta}\dot{\theta} > 0$
and				
Reverse transformation	:	$F_1 = 0$	and	$\frac{\partial \bar{D}^{\alpha+}}{\partial\sigma}\dot{\sigma} + \frac{\partial \bar{D}^{\alpha+}}{\partial\theta}\dot{\theta} < 0$
	:	$F_2 = 0$	and	$\frac{\partial \bar{D}^{\alpha-}}{\partial\sigma}\dot{\sigma} + \frac{\partial \bar{D}^{\alpha-}}{\partial\theta}\dot{\theta} < 0$

Flow rule for the two species was already defined in eqs. (53) & (54). Using, $\dot{\alpha} = -\dot{\xi}^+ - \dot{\xi}^-$, the flow rule for α can be written as,

$$\dot{\alpha} = -\dot{\xi}^+ - \dot{\xi}^- \Rightarrow \dot{\alpha} = -\dot{\lambda}^+\frac{\partial\Phi^{\alpha+}}{\partial\xi^+} - \dot{\lambda}^-\frac{\partial\Phi^{\alpha-}}{\partial\xi^-} \tag{57}$$

The evolution of the back stresses are defined through the hardening rules as,

$$\dot{\beta}^{\epsilon^t} = h_1(\epsilon^t)\dot{\epsilon}^t = h_1 H(\dot{\xi}^+ - \dot{\xi}^-) \tag{58}$$

$$\dot{\beta}^{\alpha} = h_2(\alpha)\dot{\alpha} \tag{59}$$

where $h_1(\xi^+,\xi^-)$ and $h_2(\alpha)$ are the hardening parameters due to polycrystalline and subgrain interaction effects. In order to solve for the transformation parameters, $\dot{\lambda}^+$ and $\dot{\lambda}^-$, the consistency condition for the two transformation functions, F_1 and F_2 are invoked. These conditions can be written as,

$$\dot{F_1} = \frac{\partial F_1}{\partial\sigma}\dot{\sigma} + \frac{\partial F_1}{\partial\theta}\dot{\theta} + \frac{\partial F_1}{\partial\xi^+}\dot{\xi^+} + \frac{\partial F_1}{\partial\xi^-}\dot{\xi^-} + \frac{\partial F_1}{\partial\alpha}\dot{\alpha} = 0 \tag{60}$$

$$\dot{F_2} = \frac{\partial F_2}{\partial\sigma}\dot{\sigma} + \frac{\partial F_2}{\partial\theta}\dot{\theta} + \frac{\partial F_2}{\partial\xi^+}\dot{\xi^+} + \frac{\partial F_2}{\partial\xi^-}\dot{\xi^-} + \frac{\partial F_2}{\partial\alpha}\dot{\alpha} = 0 \tag{61}$$

Inserting the expression for the stress increment $\dot{\sigma} = E(\dot{\epsilon} - \dot{\epsilon}^t)$, the transformation strain increment $\dot{\epsilon}^t = H(\dot{\xi}^+ - \dot{\xi}^-)$ and transformation flow rule into the above consistency conditions, the plastic multipliers can be solved using,

$$Ax = b \tag{62}$$

where

$$A = \begin{bmatrix} -EH\frac{\partial F_1}{\partial\sigma} + \frac{\partial F_1}{\partial\xi^+} - \frac{\partial F_1}{\partial\alpha} & EH\frac{\partial F_1}{\partial\sigma} + \frac{\partial F_1}{\partial\xi^+} - \frac{\partial F_1}{\partial\alpha} \\ -EH\frac{\partial F_2}{\partial\sigma} + \frac{\partial F_2}{\partial\xi^+} - \frac{\partial F_2}{\partial\alpha} & EH\frac{\partial F_2}{\partial\sigma} + \frac{\partial F_2}{\partial\xi^+} - \frac{\partial F_2}{\partial\alpha} \end{bmatrix}$$

$$x = \begin{bmatrix} \dot{\lambda}^{+}\bar{D}^{\alpha+} \\ \dot{\lambda}^{-}\bar{D}^{\alpha-} \end{bmatrix}$$

$$b = \begin{bmatrix} -E\dot{\epsilon}\frac{\partial F_1}{\partial \sigma} - \frac{\partial F_1}{\partial \theta}\dot{\theta} \\ \\ -E\dot{\epsilon}\frac{\partial F_2}{\partial \sigma} - \frac{\partial F_2}{\partial \theta}\dot{\theta} \end{bmatrix}$$

In the above, E is the effective elastic modulus of the the species mixture.

Solution of the Eq. (62) will yield the transformation multipliers, $\dot{\lambda}^{+}$ and $\dot{\lambda}^{-}$. Thus, the the evolution of the two species ξ^{+} and ξ^{-} can be evaluated.

The two-species evolution case (one evolving at the expense of the other) is a case where only one transformation multiplier is involved.

In the condition that both F_1 and F_2 conditions are not satisfied, one should check for the evolution of only ξ^{+} and ξ^{-} which also involves a single transformation multiplier. The simultaneous involvement of three is a more general case compared to the two species case. Therefore, the two species evolution cases are not discussed in detail here.

3. Role of parameters - Phase Diagrams

Phase diagram is a diagram that represents the existence of different phases at different conditions of stress/pressure and temperature. This is a good source for materials engineers to obtain the information about the existence of different phases under the given conditions. Early models for shape memory alloys were based on phase diagrams (see Brinson (1993); Shub and Lagoudas (1999)). It can be shown both experimentally as well as based on the proposed model that the phase diagram is dynamic in nature because it depends upon the current values of the volume fractions and not on their initial values and this can be related to the well known thermodynamics concept of path dependence. The proposed three species model, also produces entirely different transformation stress - transformation temperature diagrams which are known as phase diagrams, for different states of the material. This is discussed in detail in this section. The phase diagram which is presented in this section is purely based on the complete transformations.

To understand the role of different parameters involved in the proposed model, three different cases of dissipation and hardening are discussed in detail. To make the analysis simple, the modulus for austenite and martensite are assumed to be equal ($E_m = E_a$). The transformation functions for the forward transformations are obtained as,

$F_1 = \left|\bar{D}^{\alpha+}\right| - \bar{k_1}$ - Austenite to plus-martensite (forward)
$F_2 = \left|\bar{D}^{\alpha-}\right| - \bar{k_2}$ - Austenite to minus-martensite (forward)
$F_3 = \left|\bar{D}^{-+}\right| - \bar{k_3}$ - Minus to plus-martensite (forward)

3.1. No dissipation with Zero Hardening

If the material is assumed to be dissipationless then, ($\bar{k_1} = \bar{k_2} = \bar{k_3} = 0$). Zero hardening indicates ($\beta^{\epsilon^t} = \beta^{\alpha} = 0$). In such a condition, the transformation takes place reversibly and without hysteresis when the transformation criteria are satisfied (transformation functions reach zero). Therefore for forward transformation,

$$F_1 = \left|\sigma - \sigma^L - \beta^{\epsilon^t} + \beta^{\alpha}\right| - \bar{k_1} = 0 \Rightarrow \sigma - \sigma^L - \beta^{\epsilon^t} + \beta^{\alpha} - \bar{k_1} = 0 \Rightarrow \sigma = \sigma^L$$

$$F_2 = \left|-\sigma - \sigma^L + \beta^{\epsilon^t} + \beta^{\alpha}\right| - \bar{k_2} = 0 \Rightarrow -\sigma - \sigma^L + \beta^{\epsilon^t} + \beta^{\alpha} - \bar{k_2} = 0 \Rightarrow \sigma = -\sigma^L$$

$$F_3 = \left|\sigma - \beta^{\epsilon^t}\right| - \bar{k_3} = 0 \Rightarrow \sigma - \beta^{\epsilon^t} - \bar{k_3} = 0 \Rightarrow \sigma = 0$$

When the applied stress and temperature exceeds the value of σ^L, austenite to plus-martensite starts and ends at the same value and similarly for austenite to minus-martensite transformation occurs at $-\sigma^L$. Minus-martensite to plus-martensite transformation occurs at $\sigma = 0$ line as shown in Fig.2. Similarly for reverse

transformation,

$$F_1 = 0 \Rightarrow -\sigma + \sigma^L + \beta^{\epsilon^t} - \beta^{\alpha} - \bar{k_1} = 0 \Rightarrow \sigma = \sigma^L$$
$$F_2 = 0 \Rightarrow \sigma + \sigma^L - \beta^{\epsilon^t} - \beta^{\alpha} - \bar{k_2} = 0 \Rightarrow \sigma = -\sigma^L$$
$$F_3 = 0 \Rightarrow -\sigma + \beta^{\epsilon^t} - \bar{k_3} = 0 \Rightarrow \sigma = 0$$

the transformation starts and ends at the same stress level as shown in Fig. 2. The latent heat term, σ^L can be written in terms of stress and temperature as,

$$\sigma^L = m(\theta - \theta_o) \tag{63}$$

which is a straight line with constant slope 'm' and intersects the temperature axis at θ_o as shown in Fig.2. Values of all the material parameters assumed in this example are given in Section 6.

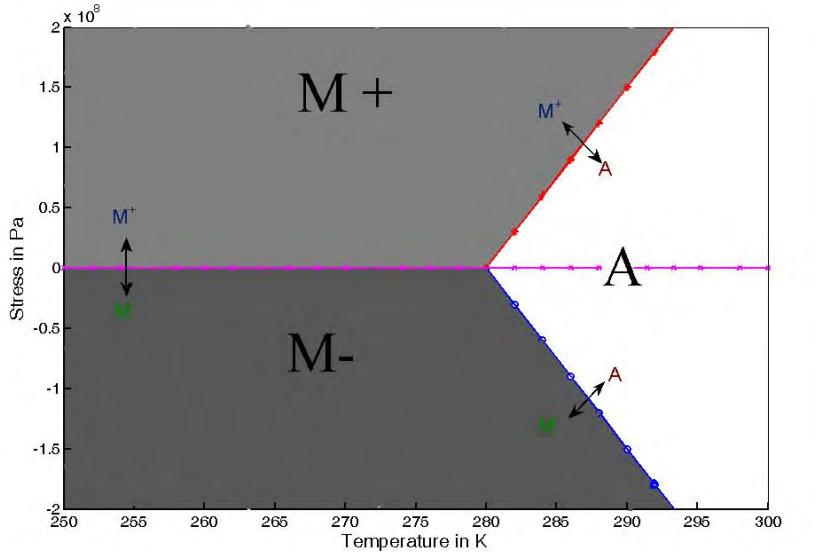

Figure 2: Zero dissipation ($\bar{k_1} = \bar{k_2} = \bar{k_3} = 0$) with out hardening ($\beta^{\epsilon^t} = \beta^{\alpha} = 0$): Phase Diagram

3.2. Dissipation with Zero Hardening

If the dissipations are take into account ($\bar{k_1}, \bar{k_2}, \bar{k_3} > 0$) with no hardening ($\beta^{\epsilon^t} = \beta^{\alpha} = 0$), from the transformation criteria, we obtain the following:
Forward transformation:

$$F_1 = 0 \Rightarrow \sigma - \sigma^L - \bar{k_1} = 0 \Rightarrow \sigma = \sigma^L + \bar{k_1}$$
$$F_2 = 0 \Rightarrow -\sigma - \sigma^L - \bar{k_2} = 0 \Rightarrow \sigma = -\sigma^L - \bar{k_2}$$
$$F_3 = 0 \Rightarrow \sigma - \bar{k_3} = 0 \Rightarrow \sigma = \bar{k_3}$$

Reverse transformation

$$F_1 = 0 \Rightarrow -\sigma + \sigma^L - \bar{k_1} = 0 \Rightarrow \sigma = \sigma^L - \bar{k_1}$$
$$F_2 = 0 \Rightarrow \sigma + \sigma^L - \bar{k_2} = 0 \Rightarrow \sigma = -\sigma^L + \bar{k_2}$$
$$F_3 = 0 \Rightarrow \sigma + \bar{k_3} = 0 \Rightarrow \sigma = -\bar{k_3}$$

Due to the presence of dissipation terms, the transformation line gets shifted from the previous case by $\pm\bar{k}$. It gives rise to six transformation lines as shown in Fig. 3.

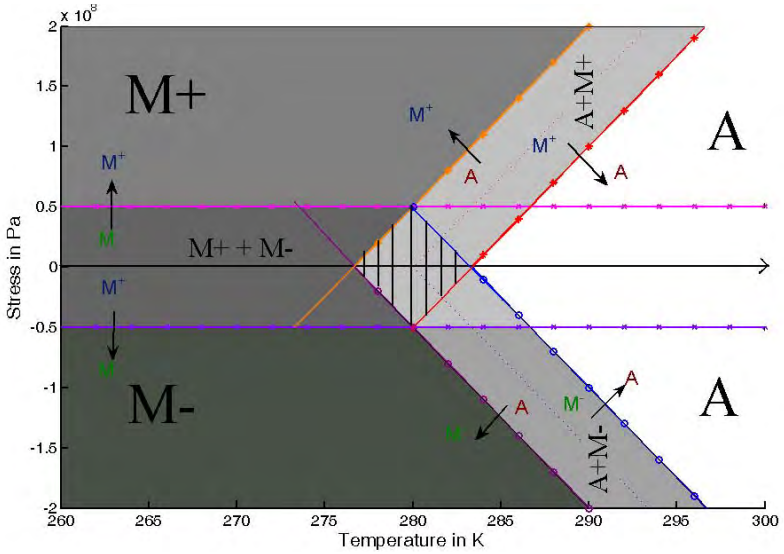

Figure 3: Non-zero dissipation ($\bar{k_1}, \bar{k_2}, \bar{k_3} > 0$) without hardening ($\beta^{\epsilon^t} = \beta^{\alpha} = 0$): Phase Diagram. The shaded regions show the existence of pure phase (darker shades) or mixtures (lighter shades). The hashed region is the region of existence of all the three species.

3.3. Dissipation with Linear Hardening

Assuming linear hardening with constant plastic modulus (h_1 and h_2), the hardening rule can be written as

$$\dot{\beta}^{\epsilon^t} = h_1 \dot{\epsilon}^t = h_1 H(\dot{\xi}^+ - \dot{\xi}^-) \tag{64}$$

$$\dot{\beta}^{\alpha} = h_2 \dot{\alpha}. \tag{65}$$

Three transformation criteria are analyzed separately in this case as follows.

F_1 - Austenite - Plus-martensite Transformation

Forward Transformation ($\alpha \longrightarrow \xi^+$)

Due to constant hardening parameters, when $\alpha = 1$, the back stress due to interaction attains a value $\beta^{\alpha} = h_2$ and $\beta^{\epsilon^t} = 0$ in the initial state itself. At the expense of α, the plus-martensite accumulates and the back stresses due to orientation β^{ϵ^t} reaches a value of Hh_1, when $\xi^+ = 1$ and β^{α} goes to zero.

$$\begin{aligned} F_1 = \sigma - \sigma^L - \beta^{\epsilon^t} + \beta^{\alpha} - \bar{k_1} = 0 \quad &\Rightarrow \quad \sigma = \sigma^L - \beta^{\alpha} + \bar{k_1} \quad \text{(starts)} \\ F_1 = \sigma - \sigma^L - \beta^{\epsilon^t} + \beta^{\alpha} - \bar{k_1} = 0 \quad &\Rightarrow \quad \sigma = \sigma^L + \beta^{\epsilon^t} + \bar{k_1} \quad \text{(ends)} \end{aligned}$$

Reverse Transformation ($\xi^+ \longrightarrow \alpha$)

During reverse transformation, β^{ϵ^t} remains at its maximum and β^{α} remains zero until transformation starts. The transformation ends at when β^{α} reaches a maximum of h_2 and β^{ϵ^t} goes to zero.

$$\begin{aligned} F_1 = -\sigma + \sigma^L + \beta^{\epsilon^t} - \beta^{\alpha} - \bar{k_1} = 0 \quad &\Rightarrow \quad \sigma = \sigma^L + \beta^{\epsilon^t} - \bar{k_1} \quad \text{(starts)} \\ F_1 = -\sigma + \sigma^L + \beta^{\epsilon^t} - \beta^{\alpha} - \bar{k_1} = 0 \quad &\Rightarrow \quad \sigma = \sigma^L - \beta^{\alpha} - \bar{k_1} \quad \text{(ends)} \end{aligned}$$

F_2 - Austenite - Minus-martensite Transformation

Forward Transformation ($\alpha \longrightarrow \xi^-$)

At the expense of α, the minus-martensite accumulates and the back stresses due to orientation β^{ϵ^t} reaches a value of $-Hh_1$, when $\xi^- = 1$ and β^{α} goes to zero, similar to the previous case.

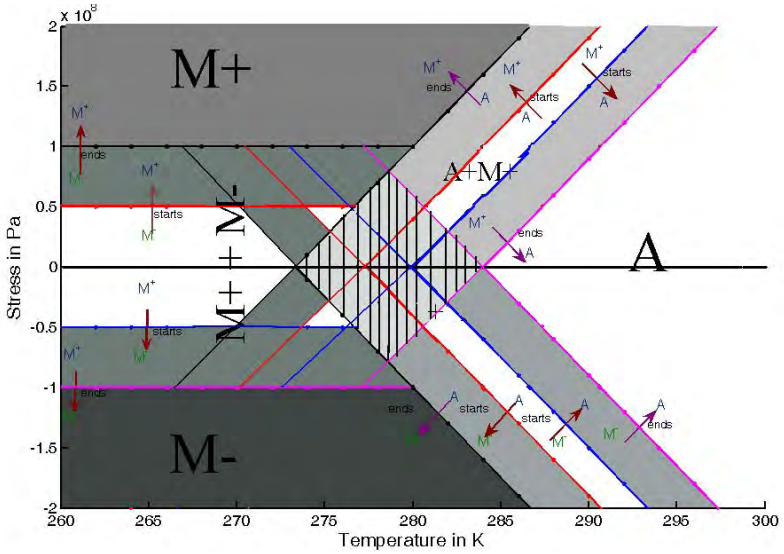

Figure 4: Non-zero dissipation ($\bar{k_1}, \bar{k_2}, \bar{k_3} > 0$) with linear hardening ($\beta^{\epsilon^t}, \beta^{\alpha} > 0$): Phase Diagram. The shaded regions show the existence of pure phase (darker shades) or mixtures (lighter shades). The hashed region is the region of existence of all the three species.

$$F_2 = -\sigma - \sigma^L + \beta^{\epsilon^t} + \beta^{\alpha} - \bar{k_2} = 0 \quad \Rightarrow \quad \sigma = -\sigma^L + \beta^{\alpha} - \bar{k_2} \quad \text{(starts)}$$
$$F_2 = -\sigma - \sigma^L + \beta^{\epsilon^t} + \beta^{\alpha} - \bar{k_2} = 0 \quad \Rightarrow \quad \sigma = -\sigma^L + \beta^{\epsilon^t} - \bar{k_1} \quad \text{(ends)}$$

Reverse Transformation ($\xi^- \longrightarrow \alpha$)
During reverse transformation, β^{ϵ^t} remains at its maximum and β^{α} remains zero until transformation starts. The transformation ends at when β^{α} reaches a maximum of h_2 and β^{ϵ^t} goes to zero.

$$F_2 = \sigma + \sigma^L - \beta^{\epsilon^t} - \beta^{\alpha} - \bar{k_2} = 0 \quad \Rightarrow \quad \sigma = -\sigma^L + \beta^{\epsilon^t} - \bar{k_2} \quad \text{(starts)}$$
$$F_2 = \sigma + \sigma^L + \beta^{\epsilon^t} - \beta^{\alpha} - \bar{k_2} = 0 \quad \Rightarrow \quad \sigma = -\sigma^L + \beta^{\alpha} + \bar{k_2} \quad \text{(ends)}$$

F_3 - Minus - Plus-martensite Transformation
The transformation starts with zero back stress (β^{ϵ^t}) and at the end of the transformation it reaches a maximum value accordingly.
Forward Transformation ($\xi^- \longrightarrow \xi^+$)
When $\xi^+ = \xi^- = 0.5$, the back stress due to orientation becomes zero. Tensile loading induces ξ^+ at the expense of ξ^- and β^{ϵ^t} reaches a maximum of Hh_1.

$$F_3 = \sigma - \beta^{\epsilon^t} - \bar{k_3} = 0 \quad \Rightarrow \sigma = \bar{k_3} \quad \text{(starts)}$$
$$F_3 = \sigma - \beta^{\epsilon^t} - \bar{k_3} = 0 \quad \Rightarrow \sigma = \beta^{\epsilon^t} + \bar{k_3} \quad \text{(ends)}$$

Reverse Transformation ($\xi^+ \longrightarrow \xi^-$)
Compressive loading induces ξ^- at the expense of ξ^+ and β^{ϵ^t} reaches a maximum of $-Hh_1$.

$$F_3 = -\sigma + \beta^{\epsilon^t} - \bar{k_3} = 0 \quad \Rightarrow \sigma = -\bar{k_3} \quad \text{(starts)}$$
$$F_3 = -\sigma + \beta^{\epsilon^t} - \bar{k_3} = 0 \quad \Rightarrow \sigma = \beta^{\epsilon^t} - \bar{k_3} \quad \text{(ends)}$$

It may be noted, this transformation function is independent of θ. Therefore, the last four lines become horizontal in the phase diagram and other eight lines inclined with a slope of $\pm m$ as shown in Fig. 4.

4. Computational Aspects

Some of the important computational steps required during the of the evolution of the state of the material system are described in this section. There are three distinct tasks that have to be carried out and they are explained in this section:
(1) Listing of all the transformation conditions for the three species.
(2) Listing of the loading criteria for each of the transformation.
(3) Listing the constraint conditions / availability checks on the species for transformation.
All these conditions have to be put together in order to determine the transformation or the evolution of a particular species.

The three yield/transformation functions derived in section 2 can be expanded to its full form and written as a system of six transformation criteria as follows:

$$
\begin{array}{lll}
F_1 = \sigma - \sigma^L - \beta^{\epsilon^t} + \beta^{\alpha} - \bar{k_1} = 0 & - & \text{Transformation criteria for } A \text{ to } M^+ \\
F_2 = -\sigma - \sigma^L + \beta^{\epsilon^t} + \beta^{\alpha} - \bar{k_2} = 0 & - & \text{Transformation criteria for } A \text{ to } M^- \\
F_3 = \sigma - \beta^{\epsilon^t} - \bar{k_3} = 0 & - & \text{Transformation criteria for } M^- \text{ to } M^+ \\
F_4 = -\sigma + \sigma^L + \beta^{\epsilon^t} - \beta^{\alpha} - \bar{k_1} = 0 & - & \text{Transformation criteria for } M^+ \text{ to } A \\
F_5 = \sigma + \sigma^L - \beta^{\epsilon^t} - \beta^{\alpha} - \bar{k_2} = 0 & - & \text{Transformation criteria for } M^- \text{ to } A \\
F_6 = -\sigma + \beta^{\epsilon^t} - \bar{k_3} = 0 & - & \text{Transformation criteria for } M^+ \text{ to } M^-
\end{array}
$$

Even though functions F_1 and F_4, F_2 and F_5 and F_3 and F_6 are complementary to each other, they have to be maintained separately to reduce the computational difficulties. For every total strain increment, the above mentioned six criteria have to be checked for finding the possible transformations. Once the transformation criteria are tested, the loading criteria should be appropriately checked to determine whether the transformation is mathematically possible or not. These are listed below.

$$
\begin{array}{llllll}
\text{Condition 1:} & F_1 > 0 & \text{and} & \Delta_1 > 0, & \text{the transformation } A \text{ to } M^+ \text{ is possible.} \\
\text{Condition 2:} & F_4 > 0 & \text{and} & \Delta_1 < 0, & \text{the transformation } M^+ \text{ to } A \text{ is possible.} \\
\text{Condition 3:} & F_2 > 0 & \text{and} & \Delta_2 > 0, & \text{the transformation } A \text{ to } M^- \text{ is possible.} \\
\text{Condition 4:} & F_5 > 0 & \text{and} & \Delta_2 < 0, & \text{the transformation } M^- \text{ to } A \text{ is possible.} \\
\text{Condition 5:} & F_3 > 0 & \text{and} & \Delta_3 > 0, & \text{the transformation } M^- \text{ to } M^+ \text{ is possible.} \\
\text{Condition 6:} & F_6 > 0 & \text{and} & \Delta_3 < 0, & \text{the transformation } M^+ \text{ to } M^- \text{ is possible.}
\end{array}
$$

where

$$\Delta_1 = \frac{\partial \bar{D}^{\alpha+}}{\partial \sigma}\dot{\sigma} + \frac{\partial \bar{D}^{\alpha+}}{\partial \theta}\dot{\theta}; \quad \Delta_2 = \frac{\partial \bar{D}^{\alpha-}}{\partial \sigma}\dot{\sigma} + \frac{\partial \bar{D}^{\alpha-}}{\partial \theta}\dot{\theta}; \quad \Delta_3 = \frac{\partial \bar{D}^{-+}}{\partial \sigma}\dot{\sigma}$$

α is taken to be the dependent variable in this computation. Therefore, after satisfying the plasticity constraints, next we have to check whether $\dot{\alpha}$ is equal to zero or not. If $\dot{\alpha} \neq 0$, F_3 and F_6 criteria are shelved, because these transformations are only possible when $\dot{\alpha} = 0$. Similarly when $\dot{\alpha} = 0$ condition is satisfied one should shelve the F_1, F_4, F_2 and F_5 transformation conditions.

In the third step, species constraint (i.e. whether within the admissible space) should be posed on all the probable transformations. This constraint gives the answer to the question whether the species is present for the reverse evolution during the transformation. It can be stated as a check on the species which is going to decrease during the transformation as to whether available or not at the beginning of the transformation. These can be stated as the following conditions.

$$
\begin{array}{ll}
\text{If } \alpha > 0 & F_1 \text{ and } F_2 \text{ are allowed to proceed} \\
\text{If } \xi^+ > 0 & F_4 \text{ and } F_6 \text{ are allowed to proceed} \\
\text{If } \xi^- > 0 & F_3 \text{ and } F_5 \text{ are allowed to proceed}
\end{array}
$$

Similarly, the transformation termination condition has to be incorporated, because the maximum possible species fraction is unity. If two of the above criteria satisfy simultaneously, it indicates the existence of all the three species.

5. Specializations

For the sake of simplicity in simulations, a few of simplifications have been made in addition to those already mentioned in the earlier sections. These simplifications, notwithstanding, the outcome of the simulations are quite consistent with the experimental observations. In this section, the simplifications made on these parameters for the ease of simulations will be elucidated in detail.

At the first level, the elastic moduli of the austenite and the martensite phases are assumed to be equal ($E_m = E_a$). In general, there are two kinds of actuators used in the practice using the shape memory alloys. One is a linear actuator and the other nonlinear. The linear actuator mainly uses only the difference in the moduli for actuation given that the stiffness change influences increase of force or stroke of the actuator while, the nonlinear actuator utilizes the pseudoelastic regime of stress-strain behavior as well, for actuation. This part of the actuator gives rise to more stroke than it's counterpart. Linear actuator, in general, utilizes very little of the transformation capability but has higher life and reliability. It's design does not need sophisticated modeling compared to the nonlinear actuator.

In the case when the difference in compliance exists and is to be taken into consideration, then, with the linear elastic assumption, the form of the term, σ^C, can be derived to be,

$$\sigma^C = \frac{1}{2H}\Delta S\sigma^2. \tag{66}$$

where ΔS is the difference between the compliance of the austenite phase and that of the martensite phase.

Because of the simplifications discussed above, the term σ^C that arises due to the difference in compliance of austenite and martensite becomes *zero* in this study. Moreover, the influence of this term is negligible in the complete transformation case that is normally studied for the nonlinear form of the actuator.

The response under tension and compression are assumed to be similar, in the sense that the maximum transformation strains ($H^+ = -H^- = H$) are the same under compression and tension. This, however, is not true going by the experimental studies Shub and Lagoudas (1999). But, this simplification is good enough in certain applications such as the actuators in the form of wires and thin rods / strips where tension application dominates.

The term in the transformation condition corresponding to the latent heat is taken as,

$$\sigma^L = m(\theta - \theta_\circ) \tag{67}$$

where 'm' is the material parameter which is the slope of the stress-temperature curve and $\theta_\circ$ is the reference temperature. The stress-temperature curve can be obtained by invoking the Clausius-Clapeyron condition.

The back stress β^{ϵ^t} is a function of ξ^+ and ξ^-. Therefore, the evolution equation for β^{ϵ^t} can be written as,

$$\dot{\beta}^{\epsilon^t} = \dot{\beta}^{\epsilon^t}(\epsilon^t) = h^{\epsilon^t}\dot{\epsilon^t} \tag{68}$$

Here, h^{ϵ^t} is assumed to be a constant. This leads to a simple linear hardening condition.
The back stress β^α is a function of α and therefore,

$$\dot{\beta}^\alpha = h^\alpha\dot{\alpha} \tag{69}$$

where h^α is taken as a constant. Note that there are two hardening parameters and their interaction need not turn out to be linear.

6. Simulation results and discussions

The simulations are carried out for a set of typical cases of thermo-mechanical loading, each to exhibit a particular feature captured by the model. The key features to be simulated are, the shape memory effect, the pseudoelastic effect and the response under an arbitrary thermomechanical loading cycle. The values of the material constants and parameters taken for the simulation are listed in the Table 1.

For the assumed hardening and dissipation constants, the following simulations are performed:

Table 1: Assumed material properties

Austenite modulus	E_a	20 GPa
Martensite modulus	E_m	20 GPa
Reference Temperature	θ_o	280 K
Stress-temperature slope	m	7.49972x10^5 Pa/K
Max.transformation strain	H	0.05
Hardening parameter 1	h_1	1000 MPa
Hardening parameter 2	h_2	10 MPa
Dissipation constants	$\bar{k_1}, \bar{k_2}, \bar{k_3}$	50 MPa

1. Isothermal mechanical loading at different constant temperatures,
2. Thermal loading under different constant stress levels, and
3. A cyclic thermo-mechanical loading

Isothermal mechanical loading is generally encountered in the pseudoelastic phenomenon when a stress-induced austenite to martensite transformation occurs. When shape memory wire is deformed in its martensite state, residual strain is induced. This process is also a case of isothermal mechanical loading. The model should be able to capture essential features of the material under these typical conditions.

Thermal loading under a constant stress is an idealization of the actuator mode under a constant bias such as, for example, lifting a weight. The stroke is effected by means of the martensite (M^+) to austenite transformation. It is important to determine the efficacy of the model to predict the stroke for different thermal loading conditions so that it can be applied efficiently in the design of a control system with an SMA actuator.

Unlike the above case, SMA actuators in real life applications have to be operated with a biasing component because of the predominant one-way mechanical stroking action (meaning that the stress-induced martensite-martensite transformation is not spontaneously reversible). Therefore, SMA actuators always come with a bias spring mechanism that enforces the initial configuration after the actuation is complete to be ready for the next actuation cycle. Such a situation calls for modeling the behavior of the SMA wire or spring under a cyclic thermomechanical loading. It is important to find out if the actuator is capable of springing back to the initial condition to work repeatably. Any residual deformation will affect the design greatly. Therefore, in the following simulations, these three typical loading cases have been considered and the model evaluated for performance.

6.1. Isothermal mechanical loading

Mechanical loading at two different constant temperatures are considered in this case. One is below M_f and the other one is above A_f. For the former case, the developed model simulates the detwinning effect with initial plus and minus martensite fractions of 0.5 each, which is consistent with the observed response at this temperature. Similarly for the high temperature case, the pseudoelastic behavior is simulated successfully. The constant temperature lines are plotted in the phase diagram as shown in Fig. 5a. During tensile loading, with $\alpha = 1$ at constant temperature yields plus-martensite after crossing a particular stress level. At this stage, the back stresses start evolving and a hardening response is seen and complete unloading brings back to $\alpha = 1$ state as shown in the stress-total strain curve in Fig. 5b. The response for the compressive loading would be as similar to the tensile loading illustrated above, because of the symmetry assumed in the simplification exercise.

6.2. Constant stress thermal loading

Given a constant stress level, fully austenite phase exists at some temperature above A_f. Cooling from that temperature at that constant stress level will initiate the transformation of austenite into different fractions of plus and minus martensite fractions depending on the magnitude of the applied stress. Cooling at zero stress forms equal amounts of plus and minus martensite as shown in Fig. 6. If the tensile stress is increased, more plus-martensite will be formed as compared to minus-martensite. Above a certain critical stress, cooling will always induce plus-martensite. Similarly, for different stress levels, heating from a temperature below M_f transforms

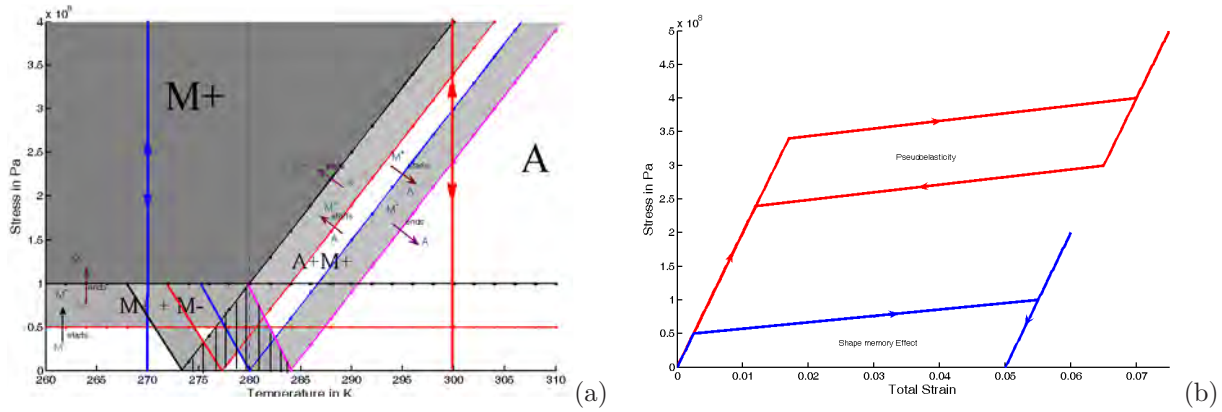

Figure 5: Isothermal loading. (a)Phase diagram for tensile loading, (b) Stress - Total strain plot. The shaded regions indicate existence of either a pure phase (darker shade or white) or mixed phases (lighter shade). The part that corresponds to the coexistence of all the three species is hashed here.

the present martensite (in any ratio of plus and minus martensite) into austenite as shown in Fig. 6. Heating and cooling below the critical stress level always involves all the three species during the transformation. Above a critical stress, either plus-martensite or minus-martensite is the only possible product along with the austenite depending on whether the applied stress is tensile or compressive.

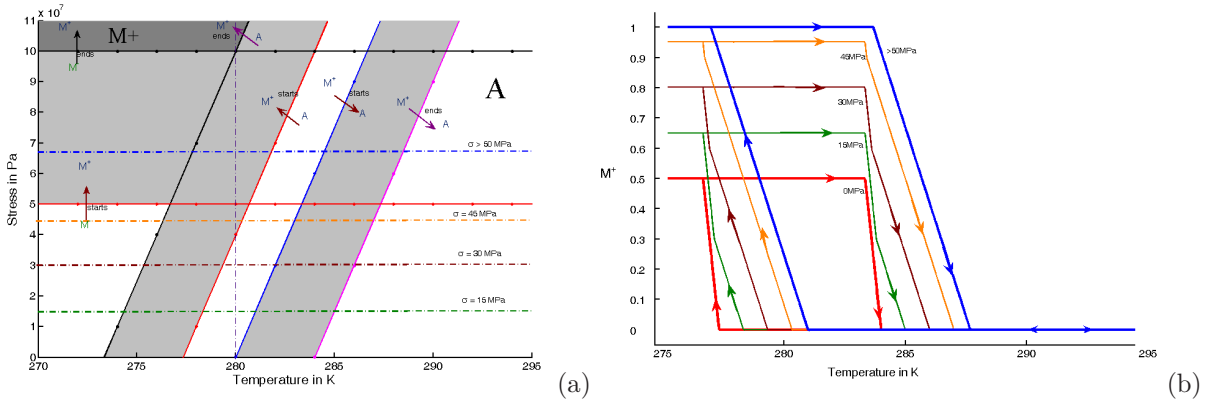

Figure 6: Thermal loading at constant temperature. (a) Phase diagram for tensile loading, (b) Temperature vs. Plus-martensite plot

6.3. Cyclic thermomechanical loading

This loading example is to explore the capabilities of this model while dealing with the arbitrary thermomechanical loading paths. In particular, this loading path is typically seen in actuator type of applications where there is a designed cycle that the material undergoes during its usage. In this example, the shape memory alloy is loaded in such a way that it is taken on a closed path across the different phase boundaries. As in the earlier example, we start from a temperature corresponding to a stress-free fully austenite phase. The material cooled, stress-free to 310 K (point S on the curve). From this point, it is loaded upto 180 MPa (point 1). It can be seen that the loading path crosses the phase boundary between S and 1, and the transformation starts here. This can be seen in Fig 7b. This is the state from which the cyclic loading starts. The cycle starts at 1, and takes the path 1-2-3-4-5 as shown in Fig. 7a. Note that in the figure, the stresses are given in Pa. The process from 1 to 2, is a

heating under a constant load until 320 K, and then a heating with increasing stress. During this transformation, the A_s phase boundary is crossed, at the point A. It can be clearly seen that the stress-strain response from 1 to A is elastic (Fig 7b). From A to 2, there is a continuous transformation, from martensite to austenite, which decreases the strain. On reaching 2, the stress is increased along with an increase in temperature upto 3. This path is purely an elastic process and does not involve any transformation. From 3, the material is cooled, and unloaded up to 4. Here, transformation starts at B, from austenite to martensite, which is associated with an increase in strain from B to 4. Unloading and cooling continues from 4 to 5 (which is the same state as 1) and here, the transformation happens at a slower rate. It can be seen that over a cyclic thermomechanical loading, the net strain change is zero, which would enable the use of this material in actuators (see Fig. 7b). This may not be the case if the hardening that is used in model does not allow the natural hysteretic memory.

7. A summary of salient features of the model

The approach followed uses the thermodynamic framework under a phenomenological setting for a polycrystalline SMA. The phenomenology is based on the generalization of a classical rate independent multiple yield surface plasticity theory. The following are the important features introduced into the model:

- A micro-mechanically motivated unified 1-D model that considers general thermo-mechanical quasi-static loading
- The ability to model partial thermo-mechanical loading/unloading cycles.
- Flexibility to introduce different transformation hardening rules, tension-compression asymmetry, etc.
- Augment other effects such as orientation effects, strain-rate dependence, fatigue, etc.
- Uses a minimal set of necessary model parameters, while being capable of simulating the complex thermo-mechanical behavior,
- Serves as a good tool for design and analysis of SMA devices, and,
- Gives pointers to avoiding redundant tests

In a one dimensional context, considering different transformation paths between the three different species viz., M^+, M^- and A, six transformation conditions are derived. The proposed framework allows for more flexibility in the specification of hardening rules. A hardening rule that considers a inner hysteresis consistent with the experimental observations is necessary. Sufficient flexibility exists, in terms of the choice of the hardening rules, latent heat functions, dissipation functions, etc. that helps fit experimental results more meaningfully and accurately. This, however, adds an additional task of devising methods to translate the experimental results into the appropriate rules and functions. Another important feature of the model is in addressing the energy associated with initial grain orientations. Additional information on orientation evolution, asymmetry of tension-compression transformation, etc. can be inserted into the model effortlessly. Temporary phase-diagrams can be constructed to illustrate the different transformation scenarios under different initial and evolving conditions of the state.

While several similarities between the proposed model and those in Lubliner and Auricchio (1996); Lagoudas *et al.* (1996) exist, there are characteristic differences. For instance, Lubliner and Aurrichio Lubliner and Auricchio (1996) use a phase-diagram to arrive at transformation surfaces to define the start and finish of any given transformation. In contrast Kumar *et al.* (2007), use the transformation surface notion to define the onset, while the finish of transformation is given by the underlying hardening law. Similarly, an analogy to derive the transformation surface from the dissipation function and a model for SMA involving two species has been proposed in Bo *et al.* (1999).

8. Concluding remarks

A three species thermomechanical model has been developed which is more amenable to the shape memory alloy design applications. The model has been formulated with capabilities that include the modeling response

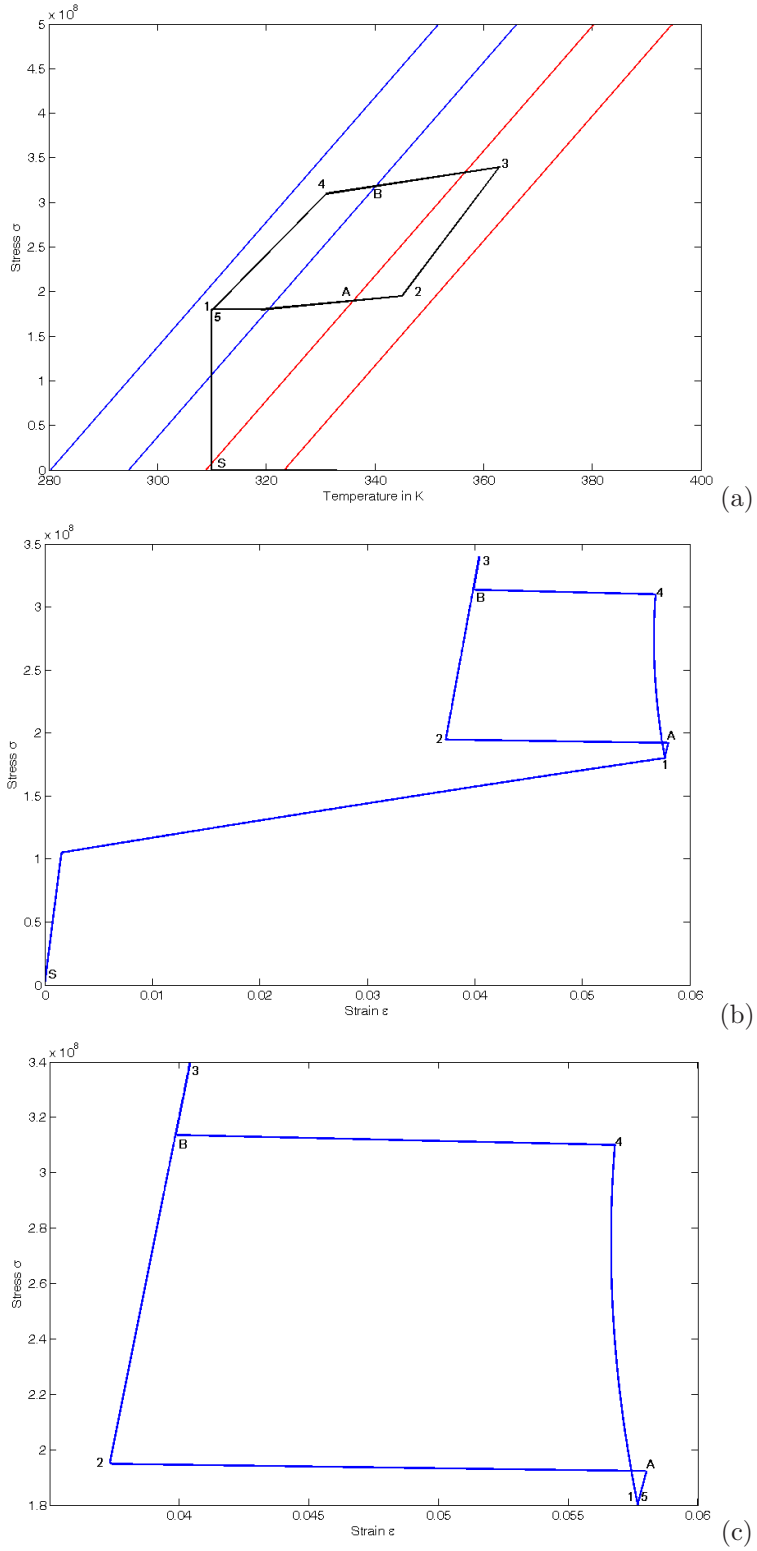

Figure 7: Cyclic loading.(a) Phase diagram , (b) Stress-strain curve for the full path, (c) Stress-strain response for the cyclic path alone. The salient points on the phase diagram have been pointed out in the response curve also.

under general thermo-mechanical loading conditions. A thermodynamically consistent formulation is adopted and this state space evolution based model serves as a good tool for different design criteria. One of the main features of this approach is its flexibility to accommodate additional variables for introducing additional effects such as plastic deformations, tension-compression asymmetry, initial texture effects, and degradation effects, that take place in the material, thus suitable for a hierarchical setting. This approach is quite designer friendly since the designer gets to pick the complexity of the model to analyze an SMA component. The modeling is micro-mechanically motivated considering the phase transformation criteria for different phase volume fractions.

It is shown, in this paper, that a minimal set of model variables used in the framework is enough to capture the salient features and provides a complete description of the one dimensional thermo-mechanical response of the SMA material. By means of illustrating the role of different model parameters, it has been shown that the basis for choice of parameter values is clearly connected to the physical response of the material. The results of the simulation for a typical loading condition (a cycle of loading for an actuation process) are shown and the various steps in the simulation are explained. A simple hardening behavior in the form of a linear hardening has been adopted for the purpose of illustration.

It is to be noted that this model has been formulated with the flexibility to change the hardening rule to suit the observed response. A more complex hardening behavior can be readily incorporated into the model for a better fit. Hysteresis can be modeled in the three species case by suitably choosing the evolution of the backstress quantities in the model.

There are, however, several other issues to be addressed, modeled and simulated such as the the two way shape memory effect observed on a trained wire or on an intentionally processed material, the R-transformations, the functional fatigue / degradation, training effects and the coupled conduction/convection, rate effects exhibited by the material. Also, it is necessary to establish a systematic procedure to the evaluate the values of the parameters and constants in the model from the experimental results. Addressing these issues forms a part of the ongoing efforts by the authors.

Acnowledgements

Authors wish to thank India Science Lab General Motors R&D, for providing funding for this work. Discussions with Prof. Arun R. Srinivasa, Dr. V. Buravalla, A. Khandelwal and Dr. P.D. Mangalgiri are gratefully acknowledged.

References

Bekker, A. and Brinson, L. (1998). Phase diagram based description of the hysteresis behavior of shape memory alloys, *Acta Materialia* **46**, pp. 3649–3665.

Bernardini, D. and Pence, T. (2002). Shape memory materials, modeling, *In: Encyclopedia of smart materials, John Wiley & Sons* , pp. 964–980.

Bo, Z., Lagoudas, D. and Miller, D. A. (1999). Material characterization of SMA actuators under nonproportional thermomechanical loading, *Journal of Engineering Materials and Technology* **121**, pp. 75–85.

Boyd, J. and Lagoudas, D. (1996). A thermodynamical constitutive model for shape memory materials. Part I The monolithic shape memory alloys, *International Journal of Plasticity* **12**, pp. 805–842.

Brinson, L. C. (1993). One dimensional constitutive behavior of shape memory alloys: Thermo mechanical derivation with non-constant material functions and martensite internal variable, *Journal of Intelligent Materials Systems and Structures* **4**, pp. 229–242.

Buravalla, V. and Khandelwal, A. (2008). A correction to the brinson evolution kinetics for shape memory alloys, *Journal of Intelligent Material Systems and Structures* **19**, pp. 43–46.

Chang, B., Shaw, J. and Iadicola, M. (2006). Thermodynamics of shape memory alloy wire: Modeling, experiments and application, *Continuum Mechanics and Thermodynamics* **18**, pp. 83–118.

Chenchiah, I. and Sivakumar, S. (1999). A two variant thermomechnaical model for shape memory alloys, *Mechanics Research Communications* **26**, pp. 301–307.

Chopra, I. (2002). Review of state of art of smart structures and integrated systems, *AIAA Journal* **40**, pp. 2145–2187.

Guthikonda, V. S. R., Kranthi, K. M., Sivakumar, S. M. and Srinivasa, A. R. (2008). On smeared and micromechanical approaches to modeling martensitic transformations in SMA, *Nonlinear Analysis-Real World Applications* **9**, pp. 990–1011.

Hill, R. (1950). The mathematical theory of plasticity, *Oxford University Press, Oxford* .

Ivshin, Y. and Pence, T. (1994). A constitutive model for hysteretic phase transition behavior, *International Journal of Engineering Science* **32**, pp. 681–704.

Kumar, M. K., Sakthivel, K., Sivakumar, S. M., Rao, C. L. and Srinivasa, A. (2007). Thermomechanical modeling of hysteresis in SMAs using the dissipationless reference response, *Smart Materials and Structures* **16**, pp. S28–S38.

Lagoudas, D. C., Bo, Z. and Qidwai, M. A. (1996). A unified thermodynamic constitutivemodel for SMA and finite element analysis of active metal matrix composites, *Mechanics of Composite Materials and Structures* **3**, pp. 153–163.

Lexcellent, C., Leclercq, S., Gabry, B. and Bourbon, G. (2000). Two way shape memory effect of shape memory alloys: an experimental study and a phenomenological model, *International Journal of Plasticity* **16**, pp. 1155–1168.

Lubliner, J. and Auricchio, F. (1996). Generalized plasticity and shape memory alloys, *International Journal of Solids and Structures* **33**, pp. 991–1003.

Ortin, J. (1992). Preisach modeling of hysteresis for a pseudoelastic cu-zn-al single crystal, *Journal of Applied Physics* **71**, pp. 1454–1461.

Otsuka, K. and Wayman, C. M. (1998). Shape memory materials, *Cambridge Univ Press, UK* .

Rajagopal, K. R. and Srinivasa, A. R. (1999). On thermomechanics of shape memory wires, *Z. Angew. Maths. Phys* **50**, pp. 459–496.

Roubicek (2004). Models for microstructure evolution in shape memory alloys, *in Nonlinear homogenization and its applications to composites, polycrystals and smart materials, P.Ponte Castaneda et al. (eds.) Kluwer Academic Publishers* , pp. 269–304.

Seelecke, S. and Muller, I. (2004). Shape memory alloy actuators in smart structures: Modeling and simulation, *Applied Mechanics Reviews* **57**, pp. 23–46.

Shub, S. and Lagoudas, D. (1999). Residual deformation of active structures with SMA actuators, *International Journal of Mechanical Science* **41**, pp. 595–619.

Smith, R. D. R. B. (2004). Shape memory alloys in seismic resistant design and retrofit: A critical review of their potential and limitations, *Journal of Earthquake Engineering* **8**, pp. 415–429.